PHYSICAL REVIEW B **77**, 081408(R) (2008)

In-line holography and coherent diffractive imaging with x-ray waveguides

L. De Caro,[1] C. Giannini,[1,*] D. Pelliccia,[2,3] C. Mocuta,[4] T. H. Metzger,[4] A. Guagliardi,[1] A. Cedola,[3] I. Burkeeva,[3] and S. Lagomarsino[3]

[1]*Istituto di Cristallografia, Consiglio Nazionale delle Ricerche (IC-CNR), via Amendola 122/O, I-70126 Bari, Italy*

[2]*Dipartimento di Fisica, Universita di Roma "La Sapienza" and INFN Sezione Roma 1, Roma, Italy*

[3]*Istituto di Fotonica e Nanotecnologie, Consiglio Nazionale delle Ricerche (IFN-CNR), via Cineto Romano 42, I-00156 Roma, Italy*

[4]*ESRF, Boîte Postale 220, F-38043 Grenoble Cedex, France*

(Received 10 January 2008; published 21 February 2008)

A Fresnel coherent diffraction imaging experiment with hard x rays is here presented, using two planar crossed waveguides as optical elements, leading to a virtual pointlike source. The coherent wave field obtained with this setup is used to illuminate a micrometric single object having the shape of a butterfly. A digital two-dimensional in-line holographic reconstruction of the unknown object at low resolution (200 nm) has been obtained directly via fast Fourier transform (FFT) of the raw data. The object and its twin image are well separated because suitable geometrical conditions are satisfied. A good estimate of the incident wave field phase has been extracted directly from the FFT of the raw data. A partial object reconstruction with 50 nm spatial resolution was achieved by fast iterative phase retrieval, the major limitation for a full reconstruction being the nonideal structure of the guided beam. The method offers a route for fast and reliable phase retrieval in x-ray coherent diffraction.

DOI: 10.1103/PhysRevB.77.081408 PACS number(s): 78.70.Ck, 42.40.−i, 42.30.Rx, 87.59.−e

Coherent x-ray diffraction imaging (CXDI) is one of the most promising techniques for studying the structure and behavior of nonperiodic single objects or nonperiodic assemblies of objects at the nanoscale. The first experiments were performed using planar incident waves.[1,2] Only recently have nonplanar waves been used with success.[3] Two striking benefits have been proved with nonplanar wave fronts: a fast convergence of the iterative phase-retrieval algorithms[4] and the possibility of measuring directly the low-q diffracted intensity (i.e., the morphological information), lost when using planar wave fields, due to the presence of a beam stop. If the incident wave field is emitted by a pointlike source, this low-q diffracted intensity pattern can contain a two-dimensional in-line magnified hologram of the unknown object, which can be recorded by an array detector.[3] However, a straightforward holographic reconstruction of the unknown object from in-line holograms is usually forbidden by the presence of the twin image pattern interfering with the object image pattern.

Another extremely important factor to consider in CXDI experiments is the degree of coherence of the incident wave. In practice, in most of the experiments, the beam that arrives onto the sample has encountered several optical elements on its path from the source, e.g., monochromators, mirrors, slits, etc., that lead to a coherence degradation at the sample position.[5] This lack of coherence can severely disturb the convergence of the phasing process, as recently discussed by Williams *et al.*[5] In this respect, a waveguide offers one of the best optical elements for producing coherent and divergent beams, both properties being extremely important for CXDI experiments.[6,7]

Recently, Fushe *et al.*[8] have performed an off-axis holographic reconstruction of a tungsten tip with a spatial resolution of about 100 nm, using hard x rays in a waveguide-based experimental setup. They used a two-beam technique with an additional reference beam to probe the phase of the diffracted wave,[9] thereby avoiding complications due to the presence of twin images of in-line holographic reconstructions. In fact, various experiments[10] have shown that holographic techniques can constitute a valid alternative to CXDI for reconstructing phase information.

In this Rapid Communication, we present an experimental setup having two planar crossed waveguides as optical elements to produce a hard x-ray virtual pointlike source used to perform an in-line holographic experiment. We show that a straightforward holographic reconstruction of the test object image, well separated by the twin image, can be obtained from the fast Fourier transform (FFT) of the recorded in-line hologram, provided that suitable geometrical conditions are guaranteed. The spatial resolution of the holographic reconstruction is limited to about 200 nm by the source size. A good estimate of the incident wave field phase can be extracted directly from FFT of the raw data, which has given us the possibility of performing very fast iterative phase retrieval at higher spatial frequencies (about 50 nm) than those of a holographic reconstruction.

The experiment was performed at the ID1 beamline of the European Synchrotron Radiation Facility (ESRF), using photons at 11 keV ($\lambda=0.1127$ nm) monochromatized by a Si(111) double crystal. A gold butterfly of maximum size of 4.6 μm and 600 nm thickness, electrochemically deposited onto a Si_3N_4 membrane, was used as test object. Figure 1 schematically shows the experimental setup used for the CXDI experiment in projection geometry. The two planar waveguides (WG1 and WG2) were made of two silicon slabs, each of 500 μm thickness, bonded together via a Microposit S1800 photoresist layer, acting as a spacer. Each waveguide is fabricated in a way to allow for an asymmetric front coupling scheme, with prereflection of the incident wave field from one of the slabs, and formation of a standing wave pattern.[7] This method permits the selection of a single mode propagating into the air-filled gap. Moreover, the 500 μm thickness of the cladding layers fully stops the direct

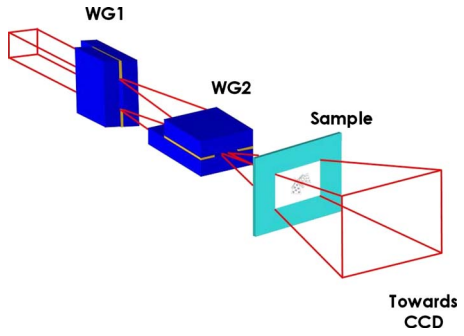

FIG. 1. (Color online) Schematic view of the experimental setup (projection geometry, not in scale).

beam, naturally avoiding the use of any additional beam stopper. The gaps of WG1 and WG2 were 290 (t_1) and 140 nm (t_2), respectively. The beam focused by beryllium lenses onto the WG1 entrance transforms into a divergent coherent linelike wave field, as schematically shown in Fig.1. This wave field propagates as a cylindrical wave onto the second planar waveguide (WG2) producing another linelike wave field perpendicular to WG1. A WG1-WG2 distance of 10 mm (d_{12}) and a WG2-sample distance of 9 mm (d_{2S}) were chosen in order to approximately satisfy the condition

$$\frac{d_{12}+d_{2s}}{d_{2s}} \approx \frac{t_1}{t_2}. \tag{1}$$

In this way, WG1 was placed at about twice the distance from the sample as WG2, to compensate for the beam divergence of the wave exiting WG1 (proportional to λ/t_1), the latter being about one-half the beam divergence at the exit of WG2 (proportional to λ/t_2). It is worth noting that, since the energy propagates within a small angle (about 0.8 mrad) to some direction (defined as the optical axis) one can apply the paraxial approximation.[11] A $W_1 \times W_2 = 10 \times 10\ \mu m^2$ area, about twice the object size, coherently illuminated the sample as required by oversampling requirements. Let us note that oversampling has to be satisfied only to allow iterative phase retrieval, the direct holographic reconstruction not requiring this condition.[8] A Princeton single-photon-counting charge-coupled device (CCD) detector with $20 \times 20\ \mu m^2$ pixel size (Δ) and 1340×1300 imaging array (PI-SX:1300) was placed at a distance $L = 3.650$ m from the sample. The combined action of the two waveguides is expected to generate an overall pointlike virtual source. In order to demonstrate this important point, we carried out the analysis of the incident beam (I_0). Figure 2(a) shows the incident beam spatial distribution at the detector plane, obtained by moving the object out of the beam path. Taking the modulus of the FFT ($\mathcal{F}$) of the incident beam, $|\mathcal{F}[I_0]|$, the autocorrelation function of the field at the exit surface of WG2 is obtained [Fig. 2(b)]. From Fig. 2(b) it follows that the source can be described effectively as being almost pointlike. Secondary maxima are present, however, whose origin is still unclear and presently under investigation. These could be due to diffraction effects of the incident wave field at the exit surfaces of the two crossed waveguides, as well as to intensity modulations of the primary beam due to the optics (mirror, monochromator).

The ratio between the intensity of the diffraction patterns measured with and without the sample in the beam path, shown in Fig. 3(a), clearly shows an in-line hologram of the test sample.

The scanning electron microscope (SEM) image of the butterfly test sample, the object to be retrieved, is shown in Fig. 3(b). Using a 600-nm-thick gold sample and working with a wavelength $\lambda = 0.1127$ nm, the first-order Born approximation[12] can be adopted to calculate the diffraction wave. In this way, the overall wave field is approximately given by the unperturbed incident wave field $A_{ref}(\boldsymbol{r})$ plus a small perturbation due to the presence of the object, $A_{scat}(\boldsymbol{r})$, where $\boldsymbol{r}$ is a vector indicating a generic point in the detector

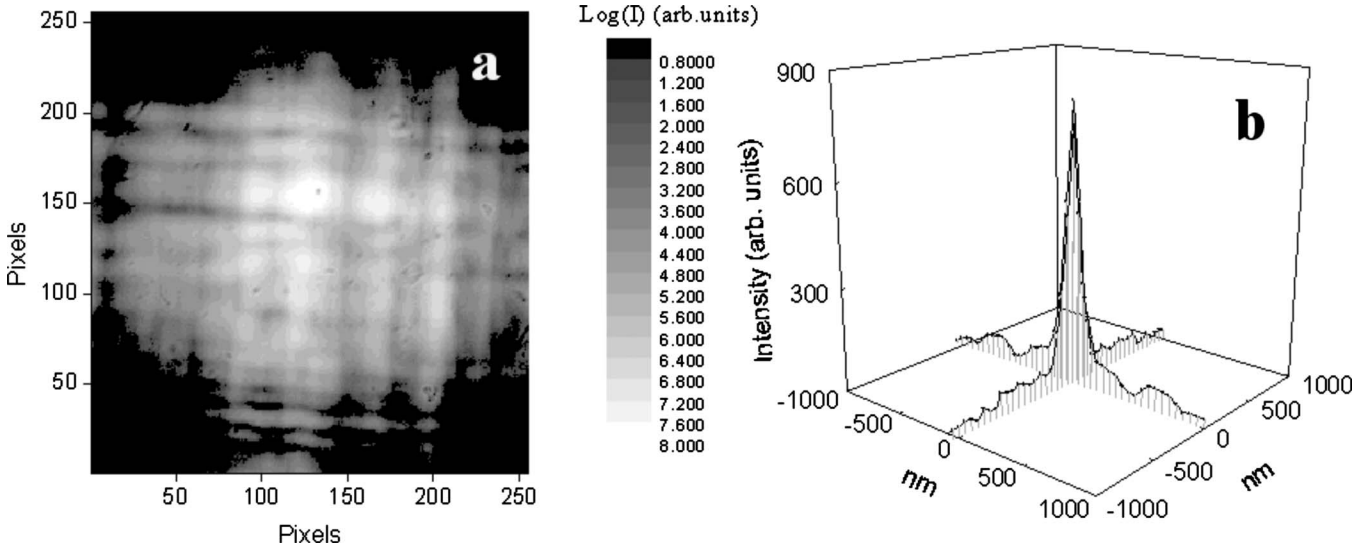

FIG. 2. (a) Measured intensity without the object; (b) three-dimensional representation of the modulus of the FFT of the raw intensity data collected without the butterfly.

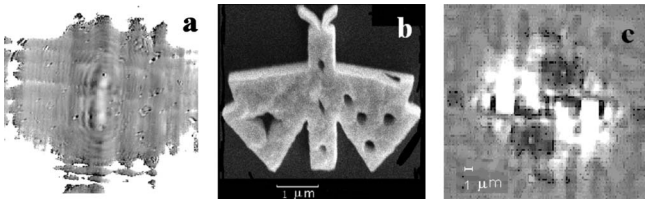

FIG. 3. (a) Ratio between diffracted intensities with and without the butterfly; (b) SEM image of the test object; (c) digital holographic reconstruction of the object image and its twin image.

plane. Indeed, at 11 keV the refractive index of a Au sample is $n=1-\delta+i\beta=1-2.4\times10^{-5}+1.4\times10^{-6}i$, and the wave field incident on a 600-nm-thick gold object is modified by a transmission function T such that $\Delta T=1-|T|=0.046\ll1$. From the two measured intensity patterns (with and without the object) we can calculate a contrast image[13]

$$I(\boldsymbol{r})=|A_{\mathrm{ref}}(\boldsymbol{r})+A_{\mathrm{scat}}(\boldsymbol{r})|^2-|A_{\mathrm{ref}}(\boldsymbol{r})|^2=\bar{A}_{\mathrm{ref}}(\boldsymbol{r})A_{\mathrm{scat}}(\boldsymbol{r})+\bar{A}_{\mathrm{scat}}(\boldsymbol{r})A_{\mathrm{ref}}(\boldsymbol{r})+|A_{\mathrm{scat}}(\boldsymbol{r})|^2, \quad (2)$$

containing a linear term in the scattered wave (holographic term), and the classical diffraction pattern (quadratic term in the scattered wave). Here, $\bar{A}$ indicates the complex conjugate. Since $\Delta T\ll1$, $|A_{\mathrm{scat}}|\ll|A_{\mathrm{ref}}|$ and the holographic term dominates in Eq. (2). The holographic reconstruction of the object image can be performed via the Kirchhoff-Helmoltz transform of Eq. (2).[14] This, in turn, can be implemented via FFT, and actually gives the autocorrelation function of the contrast intensity pattern of Eq. (2):

$$\mathcal{F}[I(\boldsymbol{r})]\approx S(\boldsymbol{u})*\bar{O}(\boldsymbol{u})+\bar{S}(\boldsymbol{u})*O(\boldsymbol{u}). \quad (3)$$

Here, the symbol $*$ indicates the convolution product; $S(\boldsymbol{u})=\mathcal{F}[A_{\mathrm{ref}}(\boldsymbol{r})]$ and $O(\boldsymbol{u})=\mathcal{F}[A_{\mathrm{scat}}(\boldsymbol{r})]$ are the source and object complex functions, respectively. For a pointlike source [$S(\boldsymbol{u})\approx\delta(\boldsymbol{u})$, with δ denoting the Dirac delta function], Eq. (3) leads to a digital holographic reconstruction of the object image plus its twin image numerically made via FFT. If the object is sufficiently shifted with respect to the optical axis, i.e., $O(\boldsymbol{u})\rightarrow O(\boldsymbol{u}-\Delta\boldsymbol{u})$ with the shift $\Delta\boldsymbol{u}$ larger than the object size, the object and its twin images are well separated in the holographic reconstruction. This condition occurred in the present experiment, as shown in Fig. 3(c). Conversely, if $\Delta\boldsymbol{u}$ had been smaller than the object size, the object image would have been superimposed on its twin image and the object would not be recognizable. The spatial resolution of the digital in-line holographic reconstruction shown in Fig. 3(c) is limited by the source size to about 200 nm. This result can be obtained thanks to the pointlike nature of the virtual source [$S(\boldsymbol{u})\approx\delta(\boldsymbol{u})$]. The secondary maxima of the source cause distortions in the holographic reconstruction of the object shape. Despite the evidenced limitations, our hard x-ray waveguide-based experimental setup has shown the possibility of performing a digital in-line holographic reconstruction of a micrometric object with a spatial resolution limited only by the source size. Prospective experiments with sources of a few tens of nanometers would allow an unknown object to

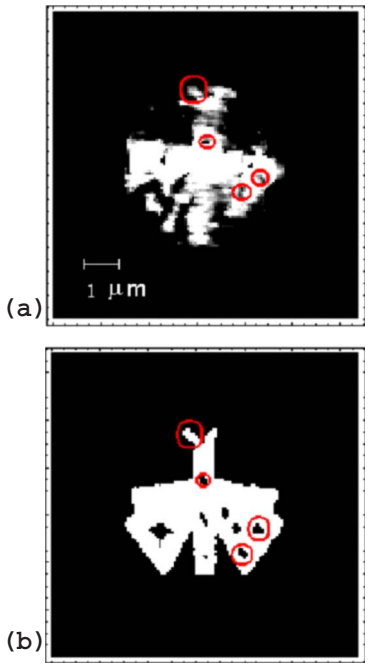

FIG. 4. (Color online) (a) Phased object; (b) one-bit SEM image of the object.

be directly extracted from the FFT of the raw data (digital holographic reconstruction) at a spatial resolution of a few tens of nanometers.

Let us note that the experimental intensity pattern contains information at higher spatial frequencies than 200 nm, corresponding to contributions of radiation scattered outside the incident wave field cone beam.[8] This further source of information can be used for a phase retrieval approach, as argued in Ref. 8, in order to reconstruct the test object at a resolution higher than the holographic one. The measured sample diffraction features are entirely contained in about half the detector size. This halves the effective numerical aperture ($\mathcal{N}_{\mathrm{eff}}$) with respect to the theoretical one (the whole CCD aperture), worsening the maximum spatial resolution at which the test object can be actually retrieved [$d=0.82\lambda/\mathcal{N}_{\mathrm{eff}}\approx50$ nm (Ref. 11)]. In this regard let us note that the CCD angular pixel size acceptance (Δ/L) does not worsen the maximum resolution, as the condition $\lambda/W_i>\Delta/L$ is satisfied.

Typically, iterative algorithms of phase retrieval from intensity data start from an estimate of the support confining the unknown object and from random phases.[3,4,15] The set of phases consistent with the measured intensity is found by recursive calculation of the propagating wave field back and forth between the object domain (where all *a priori* knowledge about the object is applied) and the Fourier domain (where the Fourier modulus of the data is applied). These iterative algorithms have been recently generalized for diffraction intensity data measured with curved coherent wave fields, in the paraxial regime, taking into account the complex illumination factors determined by the Fresnel propagators.[3,15] From our tests, we found that the FFT of the square root of the raw intensity data collected without the test sample is a complex function, whose phase is a good

approximation of the incident wave field phase, apart from a constant phase term. Starting just from the incident wave field phase so obtained and from the object low-resolution image, we used a classic error reduction phasing algorithm,[4] generalized for curved wave fields and taking into account complex illumination Fresnel factors during wave propagation in the paraxial regime.[3] In this way, a partial reconstruction of the butterfly was obtained very quickly, after only 20 iterations; it is shown in Fig. 4(a). A comparison with the one-bit SEM image of the butterfly of Fig. 4(b) indicates that many tiny features (enhanced by red circles) are present in the reconstructed image, although only a 40% correlation between the two images is found. The resolution of the partially reconstructed image is close to 50 nm, as expected. Attempts at either better retrieving the phase of the incident wave field or better retrieving the test object through several phasing algorithms,[4] more suitable for stagnant phase retrieval problems, have not led to meaningful improvements of the object reconstruction. We think that the partial reconstruction of the butterfly image can be intrinsically related to the structured guided incident wave field and does not depend on the applied algorithm. Nevertheless, as shown, the possibility of obtaining a good estimate of the wave field phase emitted by a pointlike source, directly from its autocorrelation function, is very interesting. To better understand this finding it is worth noting that, in a pointlike source complex function S, only those phases associated with the dominant amplitude (the maximum) have a big weight in determining the main features in the wave field amplitude propagation. In the limit of an ideal point source (Dirac δ function), only one phase value for the unknown function S would be needed. This property constitutes a striking benefit for any phasing retrieval process, performed on coherent diffraction data obtained with a "nearly ideal" pointlike source.

Two crossed planar waveguides in a sequential arrangement have been utilized to produce a virtual pointlike source and illuminate a micrometer-sized single object (a butterfly). This setup allows easy selection of only one propagating mode. Three results have been obtained, clearly demonstrating the benefits of this setup: (i) an image of the butterfly was straightforwardly found by a digital holographic reconstruction, with a resolution of about 200 nm (source-size limited), obtained via FFT of the raw data; (ii) phase information about the incident wave field was directly extracted from the source autocorrelation function, again thanks to the pointlike nature of the source; (iii) a very fast two-dimensional partial reconstruction of the object with 50 nm spatial resolution was achieved through an iterative phase retrieval algorithm.

Work is under way to improve the quality of the guided beam for future CXDI and in-line holography experiments.

Annamaria Gerardino is acknowledged for the electrochemical deposition of the butterfly (whose original idea is due to Nicola Catacchio) and Roberto Lassandro for his technical support during measurements.

*cinzia.giannini@ic.cnr.it

[1] J. Miao, P. Charalambous, J. Kirz, and D. Sayre, Nature (London) **400**, 342 (1999).

[2] I. K. Robinson, I. A. Vartanyants, G. J. Williams, M. A. Pfeiffer, and J. A. Piteny, Phys. Rev. Lett. **87**, 195505 (2001); J. Miao, T. Ishikawa, B. Johnson, E. H. Anderson, B. Lai, and K. O. Hodgson, *ibid.* **89**, 088303 (2002); J. M. Zuo, I. Vartanyants, M. Gao, R. Zhang, and L. A. Nagahara, Science **300**, 1419 (2003); D. Shapiro, P. Thibault, T. Beetz, V. Elser, M. R. Howells, C. Jacobsen, J. Kirz, E. Lima, J. Miao, A. M. Nieman, and D. Sayre, Proc. Natl. Acad. Sci. U.S.A. **102**, 15343 (2005).

[3] H. M. Quiney, A. G. Peele, Z. Cai, D. Paterson, and K. A. Nugent, Nat. Phys. **2**, 101 (2006); G. J. Williams, H. M. Quiney, B. B. Dhal, C. Q. Tran, K. A. Nugent, A. G. Peele, D. Paterson, and M. D. de Jonge, Phys. Rev. Lett. **97**, 025506 (2006); G. J. Williams, H. M. Quiney, B. B. Dhal, C. Q. Tran, A. G. Peele, K. A. Nugent, M. D. de Jonge, and D. Paterson, Thin Solid Films **515**, 5553 (2006).

[4] R. W. Gerchberg and W. O. Saxton, Optik (Stuttgart) **35**, 237 (1972); J. R. Fienup, Adv. At. Mol. Phys. **21**, 2758 (1982); V. Elser, J. Opt. Soc. Am. A **20**, 40 (2003).

[5] S. K. Sinha, M. Tolan, and A. Gibaud, Phys. Rev. B **57**, 2740 (1998); I. A. Vartanyants and I. K. Robinson, J. Phys.: Condens. Matter **13**, 10593 (2001); G. J. Williams, H. M. Quiney, A. G. Peele, and K. A. Nugent, Phys. Rev. B **75**, 104102 (2007).

[6] C. Fuhse, C. Ollinger, S. Kalbfleish, and T. Salditt, J. Synchrotron Radiat. **13**, 69 (2006); L. De Caro, C. Giannini, A. Cedola, D. Pelliccia, S. Lagomarsino, and W. Jark, Appl. Phys. Lett. **90**, 041105 (2007) H. M. Quiney, K. A. Nugent, and A. G. Peele, Opt. Lett. **30**, 1638 (2005).

[7] M. J. Zwanenburg, J. F. Peters, J. H. H. Bongaerts, S. A. de Vries, D. L. Abernathy, and J. F. van der Veen, Phys. Rev. Lett. **82**, 1696 (1999); D. Pelliccia, I. Bukreeva, M. Ilie, W. Jark, A. Cedola, F. Scarinci, and S. Lagomarsino, Spectrochim. Acta, Part B **62**, 615 (2007).

[8] C. Fuhse, C. Ollinger, and T. Salditt, Phys. Rev. Lett. **97**, 254801 (2006).

[9] P. Cloetens, R. Barrett, J. Baruchel, J.-P. Guigay, and M. Schlenker, J. Phys. D **29**, 133 (1996).

[10] M. Howells, C. Jacobsen, J. Kirz, R. Feder, K. McQuaid, and S. Rothman, Science **238**, 514 (1987); I. McNulty, J. Kirz, C. Jacobsen, E. H. Anderson, M. R. Howells, and D. P. Kern, *ibid.* **256**, 1009 (1992); S. Eisebitt, J. Luning, W. F. Schlotter, M. Lorgen, O. Hellwig, W. Eberhardt, and J. Stohr, Nature (London) **432**, 885 (2004); N. Watanabe, K. Sakurai, A. Takeuchi, and S. Aoki, Appl. Opt. **36**, 7433 (1997); Y. Kohmura, T. Sakurai, T. Ishikawa, and Y. Suzuki, J. Appl. Phys. **96**, 1781 (2004).

[11] M. Born and E. Wolf, *Principles of Optics*, 7th ed. (Cambridge University Press, Cambridge, England, 1999).

[12] J. M. Cowley, *Diffraction Physics*, 2nd ed. (Elsevier Science Publisher, New York, 1990).

[13] H. J. Kreuzer and R. A. Pawlitzek, Europhys. News **34**, 62 (2003).

[14] H. J. Kreuzer, K. Nakamura, A. Wierzbicki, H. W. Fink, and H. Schmid, Ultramicroscopy **45**, 381 (1992).

[15] X. Xiao and Q. Shen, Phys. Rev. B **72**, 033103 (2005).